Extraction of fractures from 3D rock images and network modelling of multi-phase flow in fracture-pore systems

Zeyun Jiang[1*], Rink van Dijke[1], Sebastian Geiger[1], Gary Couples[1], Rachel Wood[2]

1: The Institute of Petroleum Engineering, Heriot-Watt University, UK
2: School of GeoSciences, The University of Edinburgh, UK
3: International Centre for Carbonate Reservoirs

This paper was prepared for presentation at the International Symposium of the Society of Core Analysts held in Aberdeen, Scotland, UK, 27-30 August, 2012

ABSTRACT

We develop a novel method to extract pore networks from 3D rock images containing fractures, which occur in reservoir rocks such as carbonates. Similar to the medial axis for ordinary pores, a new definition of the medial surface is introduced to locate and quantify fractures. The medial surface is generated by shrinking the pore space, while preserving the topology and the main geometry of the fracture. Subsequently, the fracture is modelled by a network of virtual nodes connected by bonds that reflect its geometrical properties, such as fracture aperture, shape and connectivity with the remaining pore space. The resulting pore network model with embedded fractures is first validated by comparison of the capillary curve between different simulations. The capillary pressure curve for a distance-map based numerical simulation of mercury injection on the original pore space is compared with network simulations on systems without and with explicit embedding of the fractures, as described above, showing favourable agreement for the latter.

INTRODUCTION

Fractures exist in natural porous media such as soil and rock at a wide range of length scales from microns to several kilometres (Berkowitz, 2002). An understanding of how oil and water to move through fractures is essential for the design of oil recovery projects because if permeability of the rock matrix is extremely low the fractures will dominate the fluid flow (Neuweiler et.al. 2004).

Glass et.al. (2001) found that entrapped phase structure varies systematically with the curvature. Gu and Yang (2003) show that the interfacial profile of oil and water in fractures is strongly controlled by capillary force, viscous effect and gravity. Neuweiler et.al. (2004) point out that for a displacement process in open fractures, the in-plane curvature influences the fluid patterns significantly if the fracture aperture roughness is small compared to the mean fracture aperture. According to visualisation studies by Kapryn et.al.(2007), fracture regions with significant aperture variations enable the formation of non-wetting globules (isolated clusters), which occur in large aperture pockets with sufficient associated fracture volume, surrounded by small apertures.

Despite the above important findings, we need to further consider the mechanism of fluid flow through complex porous systems with embedded fractures, using proper methods. The Lattice-Boltzmann (LB) method has achieved big success in the simulation of fluid flow through porous media, also including fractures (Madadi and Sahimi, 2003). Similarly, Prodanović et.al. (2010) implemented the level set method to compute the location of fluid-fluid interfaces when capillary forces are dominant. However, the computational complexity has hindered a wider-range application.

By contrast, Hughes and Blunt (2001) employs a rectangular lattice of conceptual pores connected by throats to represent local aperture variations in fractures. The shortcoming of their method is that it is not practical and also has no proper criteria for defining the density of network elements in fractures. In this paper, we propose a novel approach to deal with single fractures and mixed porous systems with embedded fractures.

METHODS

For a 3D image of a rock sample containing fractures, the general workflow consists of four steps:

1. Extract medial axis and medial surfaces.
2. Measure geometrical properties.
3. Extract a mixed pore network.
4. Simulate fluid flow properties on the pore network.

Medial Surface Extraction

A commonly-used definition of the skeleton of an object comes from the grassfire transformation (Leymarie and Levine, 1992): the skeleton of a region is formed at the points where the "fire" meets after setting fire to the borders of the region. In the 3D space, a central line (medial axis) is the skeleton for a cylindrical object while a medial surface (Figure 1) is appropriate for a flaty domain. However, for example the eight edges in the middle of Figure 1 cause the formation of unwanted small sub-surfaces. In fact, we only need the central part of the surface (Figure 1(right)), which is referred to as the medial surface hereafter. Therefore, we set the following objectives:

(1) Avoid unwanted parts (see Figure 1, middle) of central surfaces of fractures;
(2) Automatically distinguish medial axis and surface in a mixed pore space;
(3) Preserve the shape and topology of pores and fractures;
(4) Keep skeleton points as central as possible;
(5) Minimise the skeleton as a point (voxel) thick.

To achieve this, we extend our previous skeletonisation algorithm (Jiang et.al. 2008) to flaty objects. The key points are to determine (I) which voxels to remove, and (II) in what order to check.

To solve (I), we use the classification by Bertrand and Malandain (1992) – simple, surface and edge points. An object point is simple if removing it does not change the topology, in other words, no connections between object points are broken and no tunnels are added as well. An object point is a surface point if no background connection exists between any two neighbours that share a face. An edge point is located on the edge of a surface, such that removing this point results in the invalidation of at least one existing surface point.

To determine the scanning order (II), the basic idea is to shrink objects from the outmost layer gradually down to the inner layers. This can be precisely prescribed by the distance map - the Euclidean distance from a pore voxel to its nearest solid voxel. In Figure 2 an artificial fracture is shown with a variety of aperture sizes and rough walls. Both are clearly represented in the extracted medial surface (Figure 2(b)). In real rocks, some fractures can be observed from images (Figure 2(c)), while in particular small fractures (Figure 2(e)) can only be revealed by the medial surfaces.

Fracture Characterisation

Fractures have many geometrical properties like aperture, orientation, height, length, area and volume, which are very important in the pore network modelling of fluid flow in fractures. Here, we only comment on the determination of apertures.

For fractures, the (half) apertures can be obtained directly as the distance values on their medial surfaces. In Figure 3, the fracture aperture distribution shows that apertures of the fracture shown in Figure 2(a) range from 2.0 µm up to 14.56 µm. In the following, we create a virtual network representing a fracture based on this distribution.

Figure 4 shows a carbonate image of 500×500×600 voxels and 46 fractures. Each medial surface is a component that is composed of connected surface and edge points. With the distance map, a surface point has a distance value as its aperture, thus each medial surface has an average aperture.

Virtual Network Generation

With the medial surface S of a fracture, a virtual network is generated by two steps: (1) create virtual nodes on the medial surface, (2) connect nodes to form virtual bonds.

For a voxel $x \in S$, let $\delta(x)$ be the Euclidean distance and define a parameter $\gamma > 0$. Then the generation of the virtual network is described as follows:

Step 1: Randomly starting with a voxel $x \in S$, mark it as a node centre. Then move to an unmarked $y \in S$ and mark it as another node centre if there is not marked voxel within the γ-ball of y (i.e. $\gamma - ball = \{u | \sqrt{(u_1 - y_1)^2 + (u_2 - y_2)^2 + (u_3 - y_3)^2} < \gamma\delta(y)$). Continues until all surface voxels have been checked.

Step 2: Set all marked voxels as being fixed and invoke the thinning algorithm without preservation of either surface or edge points. As a result, the marked points will become the virtual node centres and other voxels as bond backbones.

Step 3: Partition the fracture into network elements with balls representing nodes and segments bonds, and assign them appropriate geometric properties.

Figure 5 illustrates this process for the fracture shown in Figure 2(a), where junctions on the skeleton are regarded as node centres and segments as bonds.

CASE STUDY

We use a state-of-the-art two-phase flow network model (Ryazanov et.al. 2009) to calculate network permeabilities, capillary pressures and relative permeabilities. Flow simulations are performed on pore networks extracted from the pore space, fractures or mixed porous systems with embedded fractures.

In Figure 6, the first image shows a mixed porous system by an artificial fracture. One way to investigate the impact of the fracture on fluid flow is to simulate drainage directly on the image itself using the distance-based approach (Jiang, 2008).

First, the largest pores connected to the inlet are occupied by oil and gradually smaller pores are invaded until the fracture is filled, which corresponding to a large increase of filled pore volume. Then the simulation continues until the whole sample is invaded. During this process, we calculate the volume of invaded regions against pore inscribed radius and draw them as the circle-dotted curve in Figure 7, closely related to a capillary pressure curve. Considering fractures as normal pores, our network model gives the square-dotted curve with the input of the pore network extracted by our previous method. Finally, we extract the skeleton that consists of both medial axis and medial surface and create a mixed network. The similar curve resulting from the combined network flow simulation is drawn as triangle-dotted curve in Figure 7. It is very close to the circle-dotted curve from our distance-based simulation. We concluded that an accurate estimate the capillary pressure curve is achieved by generating a virtual network.

CONCLUSION

From a digital topology point of view, pore body and channel should be shrunk into single points and medial axis respectively, and flaty pore elements like fractures should be shrunk to medial surface while avoiding redundant edge surfaces. This has been achieved with new definitions for surface point and edge point. We have extended our distance-based thinning algorithm to generate a skeleton and automatically determine which parts of the void space should be shrunk into medial axis and which parts into medial surface. With medial surfaces as the compact representation of fractures, characterisation of fractures can then be easily done by measuring networks.

We propose a robust method to create a virtual network for a fracture, with which two critical issues have successfully addressed: (1) How many nodes need to be created, and (2) how to connect nodes by bonds. Subsequently, a more realistic network is generated for a porous media containing fractures and more accurate results have been presented.

We are now in a position to carry out several investigations: (1) analyse the effect of aperture size on the fluid flow; (2) investigate the influence of the interaction between fractures and normal pore matrix; and (3) explore the role of fracture orientation on multi-phase flow. Moreover, we are now able to distinguish the roles of fracture network from ordinary pore systems in terms of key properties like residual oil distribution during imbibitions to develop practical and effective EOR techniques.

ACKNOWLEDGMENTS

The authors gratefully acknowledge financial support from BG group and Petrobras.

REFERENCES

Berkowitz, B., "Characterizing flow and transport in fractured geological media: A review", *Advances in Water Resources*, (2002) 25, 861-884.
Bertrand, G. and G., Malandain, "A new topological classification of points in 3D images", *Lecture Notes in Computer Science*, (1992) 588, 710-714.
Glass, R.J., H., Rajaram, M.J., Nicholl, and R.L., Detwiler, "The interaction of two fluid phases in fractured media", *Colloid & Interface Science*, (2001) 6, 223-236.
Gu, Y., C., Yang, "The effects of capillary force and gravity on the interfacial profile in a reservoir fracture or pore", *Journal of Petroleum Science and Engineering*, (2003) 40, 77-87.
Hughes, R.G., M.J., Blunt, "Network modelling of multiphase flow in fractures", *Advances in Water Resources*, (2001) 24, 409-421.
Jiang, Z., K., Wu, G.S., Couples, M.I.J., van Dijke, K.S, Sorbie, J., Ma,"Efficient extraction of networks from three-dimensional porous media", *Water Resources Research*, (2007) 43, W12S03, 17. Doi:1029/2006WR005780.
Jiang, Z., "Quantitative characterisation of the geometry and topology of the pore space in 3D rock images", PhD thesis, (2008) IPE, Heriot-Watt University, UK.
Karpyn, Z.T., A.S., Grader, P.M., Halleck, "Visualization of fluid occupancy in a rough fracture using micro-tomography", *Journal of Colloid and Interface Science*, (2007) 307, 181-187.
Karpyn, Z.T., M., Piri, , "Prediction of fluid occupancy in fractures using network modelling and x-ray microtomography. I: Data conditioning and model description", *Physical Review E*, (2007) 76, 016315.
Leymarie, F., M., Levine, "Simulating the fire Transform Using an Active contour Model", *IEEE Transactions on Pattern Analysis and Machine Intelligence*, (1992) 14, 56-75.
Madadi, M., M., Sahimi, "Lattice Boltzmann simulation of fluid flow in fracture networks with rough self-affine surfaces", *Physical Review E*, (2003) 67, 026309.
Neuweiler, I., I., Sorensen, W., Kinzelbach, "Experimental and theoretical investigations of drainage in horizontal rough-walled fractures with different correlation structures", *Advances in Water Resources*, (2004) 27, 1217-1231.
Prodanović, M., S.L., Bryant, Z.T., Karpyn, "Investigating Matrix/Fracture Transfer via a Level Set Method for Drainage and Imbibition", *SPE J.* (2010) **15** (1): 125-136. SPE-116110-PA. doi: 10.2118/116110-PA.
Ryazanov, A.V., M.I.J., van Dijke, K.S., Sorbie, "Two-phase pore-network modelling: existence of oil layers during water invasion", *Transport in Porous Media*, (2009) 80, 79-99.
Valvatne, P.H., M.J., Blunt, "Predictive pore-scale modelling of two-phase flow in mixed wet media", *Water Resources Research*, (2004) 40, W07406, doi:1029/ 2003WR002627.

FIGURES

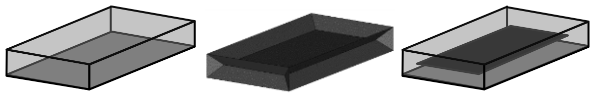

(a) (b) (c)

Figure 1. Using normal grassfire transformation, a 3D object (a) can be shrunk to a medial surface (b) in comparison with our targeting fracture surface (in black, (c)).

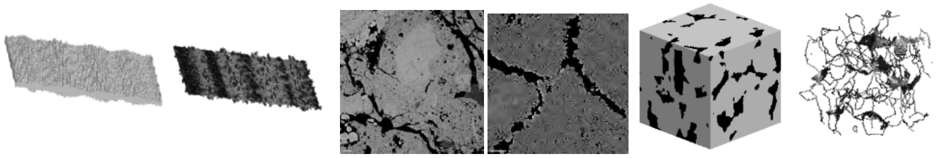

(a) (b) (c) (d) (e)

Figure 2. An artificial fracture (a) and its medial surface (b), carbonate rocks with fractures (c), sandstone image (d) and its skeleton (e). The different grey levels are used in (b) and (e) to represent the distribution of the Euclidean distances from skeleton voxels to their closest solid voxels.

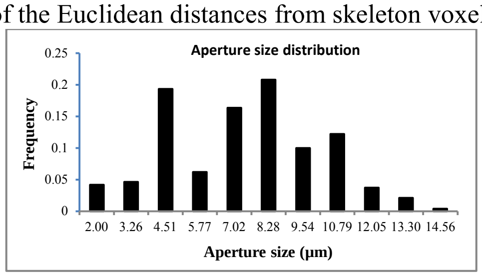

Figure 3. The aperture distribution of the fracture shown in Figure 2(a).

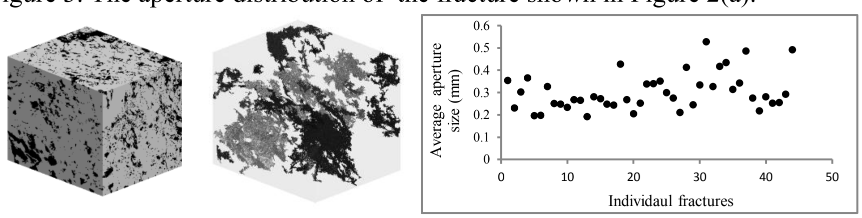

Figure 4. (a) A μ-CT tomograph of a carbonate at resultion of 48 μm and (b) the medial surfaces of 46 fractures in different grey levels, (c) a scatter plot of average apertures for the fructures.

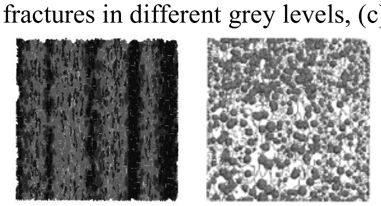

Figure 5. The medial surface of the fracture shown in Figure 2(a), and its virtual network.

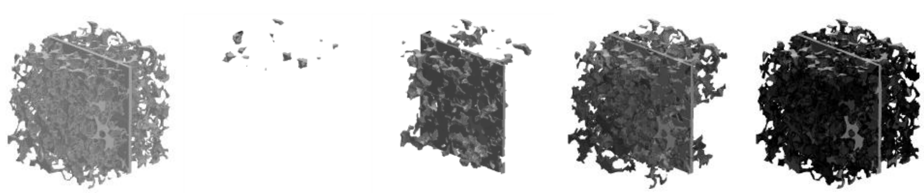

Figure 6. A mixed porous system embeded with an artificial fracture. And visualisation of distance-based simulation of drainage (downwards), showing the non-wetting phase varying from large pores (light grey) to small pores (dark grey).

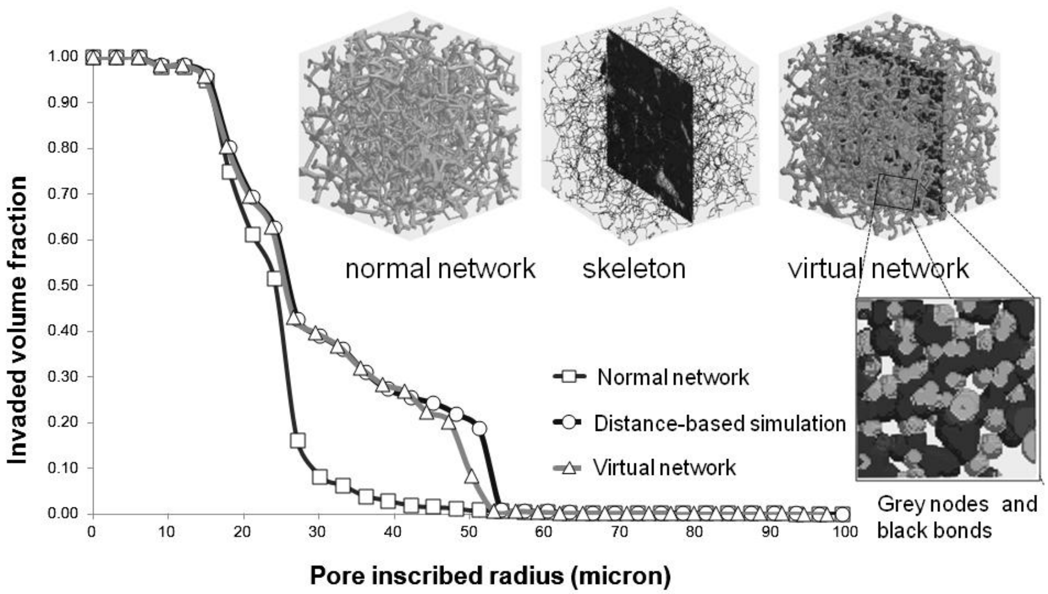

Figure 7. Filling curves for drainage into the mixed porous system shown in Figure 6, from network flow simulation on "normal" and "virtual" networks, as well as from a distance-based simulation.